Neuroscience 582 (2025) 1–10

Contents lists available at ScienceDirect

Neuroscience

journal homepage: www.elsevier.com/locate/nsc

Research Article

A cross-subject MDD detection approach based on multiscale nonlinear analysis in resting state EEG

Zhen Zhang [a], Jianli Yang [a,b,c,*], Peng Xiong [a,b], Huaqing Hao [a,b], Jieshuo Zhang [a,b], Licong Li [a,b], Changyong Wang [d], Xiuling Liu [a,b,*]

[a] *College of Electronic Information and Engineering, Hebei University, Baoding 071002, China*
[b] *Key Laboratory of Digital Medical Engineering of Hebei Province, Baoding 071002, China*
[c] *Academy of Medical Engineering and Translational Medicine, Tianjin University, Tianjin 300072, China*
[d] *Department of Neural Engineering and Biological Interdisciplinary Studies, Institute of Military Cognition and Brain Sciences, Academy of Military Medical Sciences, Beijing 100850, China*

A R T I C L E I N F O

Keywords:
Resting state EEG
MDD
Multiscale
Cross-subject

A B S T R A C T

Exploring multi-scale nonlinear patterns from different frequency bands in resting state electroencephalogram (EEG) signals is significant for major depressive disorder (MDD) detection. The study aims to investigate potential EEG biomarkers and realize cross-subject detection of MDD. This study used multiscale LZC (MLZC) to extract nonlinear features of resting state EEG. Brain topography analysis was used to investigate the difference between MDD and healthy controls (HC) among different scales. A multiscale feature fusion method was proposed to realize the cross-subject detection of MDD. Two public datasets (MPHC and MODMA) and three classifiers were used to validate the performance of the proposed method. Compared with other scales, the difference between the two groups was larger in the high frequency scale, as demonstrated by the higher complexity of brain activity in the HC group than in the MDD group. For the classification, the high frequency scale LZC had the best classification results, with accuracies of 68.75%, 82.61%, and 73.44% in MODMA, MPHC, and fused datasets. Through the multiscale feature fusion analysis, it is found that it retains a large amount of high-frequency channel information for the three datasets, highlighting the importance of high frequency features. By combining the multiscale nonlinear feature fusion, it achieves the best classification results on the three dataset experiments, with accuracies of 72.42%, 84.81%, and 76.13%, respectively. The high frequency scale LZC is more effective for MDD diagnosis in resting state EEG. The cross-subject MDD patients detection accuracy can be promoted by multiscale nonlinear feature fusion.

Introduction

Major depressive disorder (MDD) is a prevalent psychiatric disorder with clinical features including low mood, diminished interest, fatigue, and impaired cognitive function (Malhi and Mann, 2018). According to epidemiological research, large-scale surveys indicate a sharp rise in the global prevalence of depression (COVID-19 Mental Disorders Collaborators. , 2021). WHO data indicate that depression is among the primary causes of disability globally. Conventional diagnostic methods for MDD rely heavily on clinical interviews and self-report scales (e.g., Hamilton Depression Scale, Beck Depression Inventory), but these approaches are influenced by subjective reporting and clinician expertise, introducing variability (Zimmerman et al., 2015). EEG, a non-invasive tool with high temporal resolution for neurophysiological monitoring, has found extensive applications in emotion cognition research (Sun et al., 2025; Li et al., 2024) and clinical diagnosis of psychiatric disorders (Anik et al., 2024).

EEG analysis technologies have shown significant promise in advancing the diagnosis of MDD in recent years. Researches have demonstrated marked differences in EEG signals between individuals with MDD patients and healthy controls, with frequency band data revealing functional and abnormal brain patterns across states. For example, MDD patients often exhibit decreased alpha band (8–12 Hz) activity, especially in the prefrontal cortex (Yang et al., 2023); some studies have found a notable correlation between frontal alpha asymmetry (FAA) and MDD, particularly for FAA (F4 − F3) (Luo et al., 2025),

* Corresponding authors at: College of Electronic Information and Engineering, Hebei University, Baoding 071002, China.
E-mail addresses: yangjianli_1987@126.com (J. Yang), liuxiuling121@hotmail.com (X. Liu).

https://doi.org/10.1016/j.neuroscience.2025.07.020
Received 28 March 2025; Accepted 10 July 2025
Available online 12 July 2025
0306-4522/

while elevated theta band (4–8 Hz) activity may correlate with cognitive suppression (Pratiwi, 2023). Additionally, gamma band (30–100 Hz) irregularities often appear in the EEG of individuals with MDD, highlighting its strong association with cognition and emotion regulation (Lan et al., 2023). In the context of MDD research, irregularities in high frequency EEG signals, particularly gamma waves, are believed to be strongly linked to emotional disturbances, cognitive impairments, and neural network dysfunction. Evidence indicates that gamma wave activity in individuals with MDD may be inhibited or show changes in complexity, highlighting difficulties in emotional regulation and cognitive control (Zhang et al., 2022).

Since high frequency band information is closely related to cognitive function and emotion regulation, and most of the research focused on the abnormalities of high frequency band information has been carried out under paradigms such as emotional stimulation, insufficient attention has been paid to multiple frequency bands of information, especially high frequency band information, in the resting state, which affects the conclusions of diagnostic analyses of MDD (Tatti et al., 2024). Individual differences need to be taken into account in clinical diagnosis, but single band information may not be sufficient to cover the pathophysiological characteristics of all individuals (Wang et al., 2023). Therefore, in order to improve the accuracy and reliability of MDD diagnosis, it is recommended that multi bands analysis method be used to construct a more comprehensive diagnostic model by combining information from different frequency bands. This can better reflect the complexity of MDD and take into account the differences between individuals, thus improving the generalization ability of cross-subject diagnosis (Xu et al., 2024; Ke et al., 2024).

In recent years, EEG multi bands information studies have made remarkable progress in revealing the neural mechanisms of MDD, and more and more studies have shown that EEG features in multi bands can be used as important biomarkers of MDD. For example, Zhu et al. (Zhu et al., 2023) proposed an EEG signal analysis method based on convolutional neural networks, fast fourier transform (FFT), and empirical mode decomposition (EMD) algorithms to explore the classification performance of theta, alpha, and beta bands in MDD diagnosis. He et al. (He et al., 2023) examined resting state gamma rhythm abnormalities and theta-gamma coupling patterns, suggesting their utility as key diagnostic biomarkers for MDD. Liang et al. (Liang et al., 2022) explored the impact of depression on occipital alpha bands and frontal theta bands in EEG, emphasizing their significance in temporal perception and cognitive tasks. Current research often applies frequency domain features to analyze resting state EEG signals, but the nonlinear and dynamic properties of EEG make it difficult for these methods to capture the full scope of information.

Complexity analysis plays a crucial role in understanding brain diseases by revealing the dynamic and nonlinear characteristics of brain activity. Abramov et al. (Abramov et al., 2024) established a statistical model of attention-deficit/hyperactivity disorder (ADHD) by analyzing the complexity of brain electrical signals. Angulo-Ruiz et al. (Angulo-Ruiz et al., 2023) analyzed the multi-scale entropy (MSE) of ADHD EEG and found it to be lower compared to the normal group, and by analyzing the resting-state EEG of children with autism spectrum disorder (ASD), they discovered that compared to normal children, ASD children have lower complexity at higher scales (Angulo-Ruiz et al., 2023). Lord et al. (Lord and Allen, 2023) compared the sample entropy (SampEn) and Higuchi fractal dimension (HFD) values of MDD patients and found them to be lower than those of the control group. Lempel-Ziv Complexity (LZC), a nonlinear complexity metric based on information theory, effectively measures the complexity of EEG signals (Lempel and Ziv, 1976). Yang et al. (Yang et al., 2023) found that the LZC values of MDD were higher than those of the HC group. However, the results were only verified at a single scale, and the nonlinear features of EEG at different frequency bands may reflect different types of brain activity, and the complexity features may also be different.

For the above problems, this study proposes multiscale LZC (MLZC) analysis method to extract the dynamic nonlinear features of EEG from different scales, and to explore the influence of different scales of nonlinear information in resting state EEG signals on the diagnostic effect of MDD in the resting state. The MLZC fusion and selection (MLZC-FS) method is proposed to fuse and select the LZC features in various scales to comprehensively capture the effective nonlinear information on various frequency bands in the brains of MDD patients. Validated under cross-subject diagnostic experiments with multiple datasets and different classifiers to ensure the validity and stability of the experimental method, which is more applicable to the problem of assisted diagnosis of clinical depression.

Materials and methods

Dataset

In this study, we used two publicly available EEG datasets: the MPHC dataset and the MODMA dataset.

The MODMA dataset (Cai et al., 2022), sourced from the School of Information Science and Engineering, Lanzhou University, includes 5 min resting EEG signals for 24 depressed patients (13 males and 11 females; 16–56-year-old) and 29 healthy controls (20 males and 9 females; 18–55-year-old), the age and gender ratio are similar in the two groups. All MDD patients met the diagnostic criteria for major depression of the Diagnostic and Statistical Manual of Mental Disorders (DSM) based on the DSM-IV, all patients diagnosed and selected by professional psychiatrists in hospitals. For MDD patients, no psychotropic medication was administered in the past two weeks. For the control group, those who had abused or been dependent on alcohol or psychotropic substances in the past year were excluded. EEG signals in this dataset were recorded using 128 electrodes at a sampling frequency of 250 Hz. The dataset collection adhered to the ethical guidelines of the World Medical Association's Declaration of Helsinki, with all participants signing informed consent forms.

The MPHC dataset (Mumtaz et al., 2017), collected by the Centre for Intelligent Signal and Imaging Research (CISIR) at Universiti Teknologi PETRONAS, Malaysia, includes 5-minute EEG recordings of 34 major depressive disorder patients (17 males and 17 females, mean age = 40.3 ± 12.9) and 30 healthy controls (HC) (21 males and 9 females, mean age = 38.3 ± 15.6) in resting states with eyes closed and eyes open. The age ratio is similar in the two groups. The MDD patients met the internationally recognized diagnostic criteria for depression, named as DSM-IV. The MDD patients had gone through a washout time period of two weeks before commencing the EEG recording. The healthy participants were examined for psychiatric conditions and were found healthy. MDD group and control groups were positioned in a semi-reclined seating posture. EEG signals in this dataset were recorded using 19 electrodes following the international 10–20 system, with a sampling frequency of 256 Hz. All participants provided informed consent, and the study design and data collection were approved by the Hospital Universiti Sains Malaysia (HUSM) Ethics Committee.

Data preprocessing

In this study, EEG data preprocessing was conducted using EEGLAB. During the preprocessing of the MODMA dataset, 19 channels identical to those in the MPHC dataset were selected from the original 128 electrodes for consistency. The electrode layout is shown in Fig. 1. Bad channels were removed by observing waveforms, interpolated using the average of surrounding channels, re-referenced to an average reference, and filtered with a finite impulse response filter at 0.1 Hz high pass and 45 Hz low pass to reduce power line interference. The raw EEG signals collected contained various artifacts affecting signal analysis. These data were independent and typically followed a non-Gaussian distribution (Maddirala and Shaik, 2018), allowing independent component analysis (ICA) to separate them into independent components. Therefore, ICA

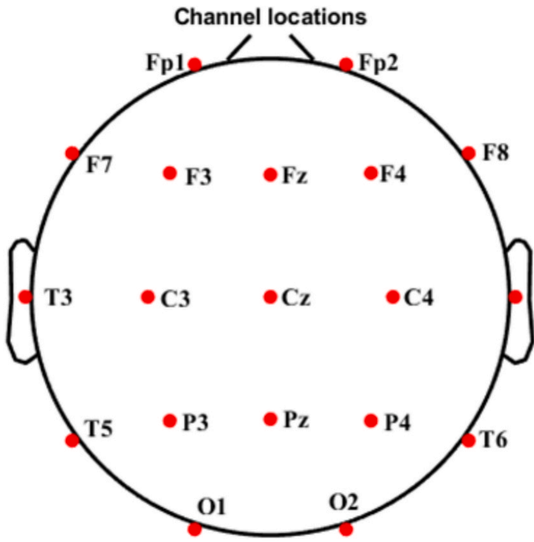

Fig. 1. Nineteen-channel brain electrode distribution map.

tools in EEGLAB were used in this study to remove artifacts such as ocular and muscular activity. Finally, bad segments of EEG signals were manually removed.

To ensure consistency with the task paradigm of the MODMA dataset, we only selected the resting state with eyes closed data from the MPHC dataset. Except for this difference, all preprocessing procedures mirrored those performed on the MODMA dataset.

According to the International 10–20 system, the brain regions are divided, as shown in Table 1. Electrodes can be divided into frontal, temporal, central, and parietal-occipital brain regions, which can be better analyzed by the brain region.

Finally, for the MODMA dataset, there were 29 HC and 24 MDD patients, each with 4 min of the resting state with eyes closed data. The data were divided into 10 s segments, resulting in 696 segments for healthy controls and 576 segments for MDD patients. For the MPHC dataset, due to insufficient data after processing for some healthy controls and MDD patients, 25 healthy controls and 24 MDD patients were finally selected. After segmenting the data, each participant had 4 min of the resting state with eyes closed data. The data were divided into 10 s segments, resulting in a total of 600 segments for the healthy control group and 576 segments for the MDD patient group.

Multiscale dynamic EEG features extraction

MLZC was used to characterize the dynamic process of EEG signals in different scales. The calculating process is divided into two main steps, sequence binarization and computational complexity. Different from the traditional approach is the binarization process.

The calculation method described by Kaspar and Schuster (Kaspar and Schuster, 1987) uses a single threshold to binarize the EEG signal and then applies LZC to analyze the patterns in the binary sequence. The calculation formula is shown in Equation (1); where m represents the median of the segment, resulting in the binarized sequence S from the EEG signal X ($x(1),\ldots, x(r),\ldots, x(N)$).

Table 1
Brain region division based on the 10–20 International EEG system.

Brain region	Channels
Frontal	Fp1, Fp2, F3, and F4
Temporal	F7, F8, T3, T4, T5, and T6
Central	C3, C4, Fz, Cz, and Pz
Parietal-Occipital	P3, P4, O1, and O2

$$s(n) = \begin{cases} 0, x(r) \le m \\ 1, x(r) > m \end{cases} \tag{1}$$

After obtaining the binary sequence S, the sequence is scanned from left to right to count the number of distinct patterns. Each time a new pattern is identified, the complexity value increments. A detailed description of this algorithm can be found in (Kaspar and Schuster, 1987).

However, traditional binarization faces significant limitations when applied to EEG signals with fast rhythms. Its threshold calculation over the entire data segment results in data loss during conventional binarization, particularly of rapid rhythm information essential for brain function characterization. In this study, we used a multiscale approach to analyze the complexity of EEG signals, based on the improvements proposed by Ibáñez-Molina et al. (Ibáñez-Molina et al., 2015), aiming to overcome the limitations of traditional method in handling rapid EEG rhythms.

For an EEG signal X ($x(1), x(2),\ldots, x(N)$) with frequency W, each point has a unique threshold $Td_k(n)$, calculated as shown in Equation (2):

$$Td_k(n) = \text{median}\ (x\left(n - \tfrac{H_k - 1}{2}\right), \cdots, x(n), \cdots, x\left(n + \tfrac{H_k-1}{2}\right))$$

$$n = 1 + \frac{H_k - 1}{2}, \cdots, +N - \frac{H_k - 1}{2} \tag{2}$$

Here, H_k is the window length used for frequency k, calculated as shown in Equation (3):

$$H_k = \frac{W}{k} \tag{3}$$

The original EEG signal is smoothed using a window length H_k to obtain the threshold Td_k for each point, followed by binarization as detailed in Equation (4):

$$y(n) = \begin{cases} 0, x(n) \le Td_k(n) \\ 1, x(n) > Td_k(n) \end{cases} \tag{4}$$

After the computation a binary sequence Y consisting of y(n) is obtained, its LZC calculated, and the value normalized. Normalization operation refers to the related research (Ibáñez-Molina et al., 2015), specifically as shown in Equation (5), where LZC_w represents the LZC value in the scale corresponding to frequency W, N_LZC_w denotes the normalized feature value, and N is the length of this sequence segment.

$$LZC_w = \frac{LZC_w}{N/log_2N}$$

We demonstrated this method using a subset of EEG data from the dataset, with comparative results shown in Fig. 2. Signal represents the EEG signal, TdN is the threshold (median) for the entire EEG segment, $Td9$ is the threshold for EEG with a step size of 9, and $P9(n)$ and $PN(n)$ are binary sequences processed using traditional and improved binarization methods, respectively. From the figure, it is evident that using window smoothing to calculate binary thresholds, higher frequencies correspond to shorter windows, allowing the capture of rapid signal changes and preserving high frequency complex activity information.

In this study, the selection of binarization windows follows literature recommendations. For instance, in the MPHC dataset with a 250 Hz sampling rate, to identify the appropriate step size for the delta band (0.1–4 Hz), according to the definition of MLZC, H_k was set to 125 (250 Hz/2Hz). For the MODMA dataset with a 256 Hz sampling rate, Hk was set to 128 (256 Hz/2 Hz). However, as the step size must be an odd number, and larger smoothing windows can include the patterns of slightly shorter windows (Ibáñez-Molina et al., 2015), we ultimately chose a window length of 131 to represent the delta scale (2 Hz). Using the same method, the step sizes for the theta scale (4 Hz), alpha scale (10 Hz), beta scale (13 Hz), and gamma scale (30 Hz) were set to 43, 27, 21, and 9, respectively. This approach enables the analysis of EEG signal complexity across different frequency bands, capturing the complexity

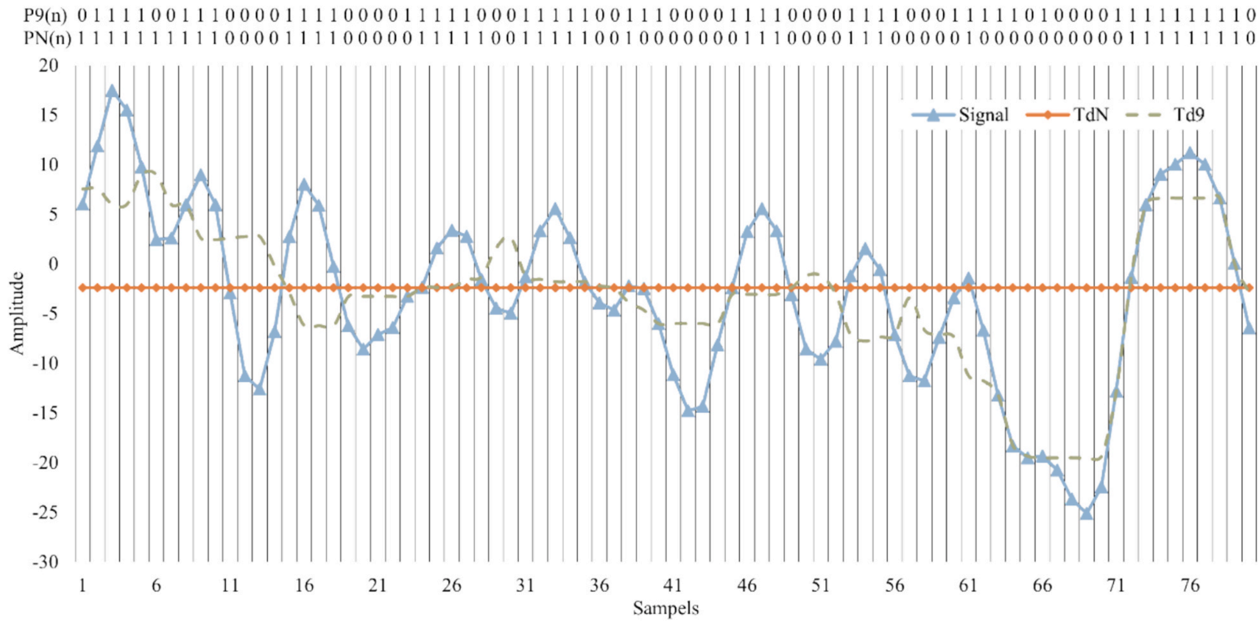

Fig. 2. Comparison of the binarization process of conventional LZC and MLZC.

of rapid components often overshadowed by slower rhythms in LZC calculations. It allows for a more detailed examination of brain oscillation patterns, which is critical for understanding brain states and functions.

The values of MLZC directly reflects the complexity of EEG signals in different frequency bands. An increase in complexity at a specific scale may indicate enhanced brain activity or the presence of a specific brain state. Conversely, a decrease in complexity at a specific scale might suggest reduced brain activity or changes in brain state. By analyzing complexity changes across different scales, we can more comprehensively investigate differences in brain activity between MDD patients and healthy control groups.

Feature fusion and classification

In this study, MLZC features were fused by concatenation. Because of the fusion of multiscale features, many of which may be irrelevant to the target, feature selection is particularly important for such high-dimensional data. The relief algorithm is a feature selection method that assigns weights to features based on their correlation with the target variable, identifying features most helpful for classification (Kononenko, 1994). In this study, the relief algorithm was used to assess the correlation between features and EEG signal class labels, identify features beneficial for EEG classification, remove irrelevant or redundant features, and reduce model complexity.

Three widely used machine learning algorithms, Support Vector Machine (SVM), K Nearest Neighbors (KNN), and Decision Tree (DT), were used in this study to carry out the MDD classification in this study. SVM is a supervised machine learning method that is widely used for classification and regression. To solve classification problems involving two modalities, it finds the best hyperplane in the feature space. New data are mapped to the same space and classified according to which side of the plane they fall on (Cortes and Vapnik, 1995). KNN is a nonparametric statistical classification and regression method based on a space vector model. KNN is based on the principle of measuring the distances between the eigenvalues of different samples, where neighboring samples have a high degree of similarity. Therefore, the new sample belongs to the category with the highest number of occurrences in the last k samples (Cover and Hart, 1967). DT is a nonparametric supervised learning method for classification and regression. DT can infer the classification rules of a decision tree from a set of irregular elements and use them to classify data (Quinlan, 1986).

Evaluation indicators

To validate the experimental results, three performance evaluation metrics are considered in this study. In the binary classification problem, the samples are categorized into four cases: true positive (TP), false positive (FP), true negative (TN) and false negative (FN) according to the prediction and actual labeling of the samples. Then the confusion matrix for binary classification is obtained as shown in Table 2.TP represents the number of correctly categorized subjects with MDD. FP represents the number of healthy controls categorized as depressed. TN represents the number of correctly categorized healthy controls. FN represents the number of subjects with MDD categorized as healthy controls. From this matrix, sensitivity, specificity and accuracy can be obtained. The corresponding calculations are shown in equations (6) (7) (8):

$$sensitivity = \frac{TP}{TP + FN} \tag{6}$$

$$specificity = \frac{TN}{FP + TN} \tag{7}$$

$$accuracy = \frac{TP + TN}{TP + TN + FP + FN} \tag{8}$$

Cross-subject experiment design

In order to validate the reliability and stability of the method, this paper conducts cross-subject experiments on two datasets. As shown in Fig. 3, HC represents healthy controls and MDD represents patients with major depressive disorder, the following are the specific experimental methods:(1) When conducting cross-subject experiments on the two datasets separately, the population of MDD and HC on each dataset is

Table 2
Confusion matrix for the classification problem.

	Predicted:Positive	Predicted:Negative
Actual:Positive	TP	FN
Actual:Negative	FP	TN

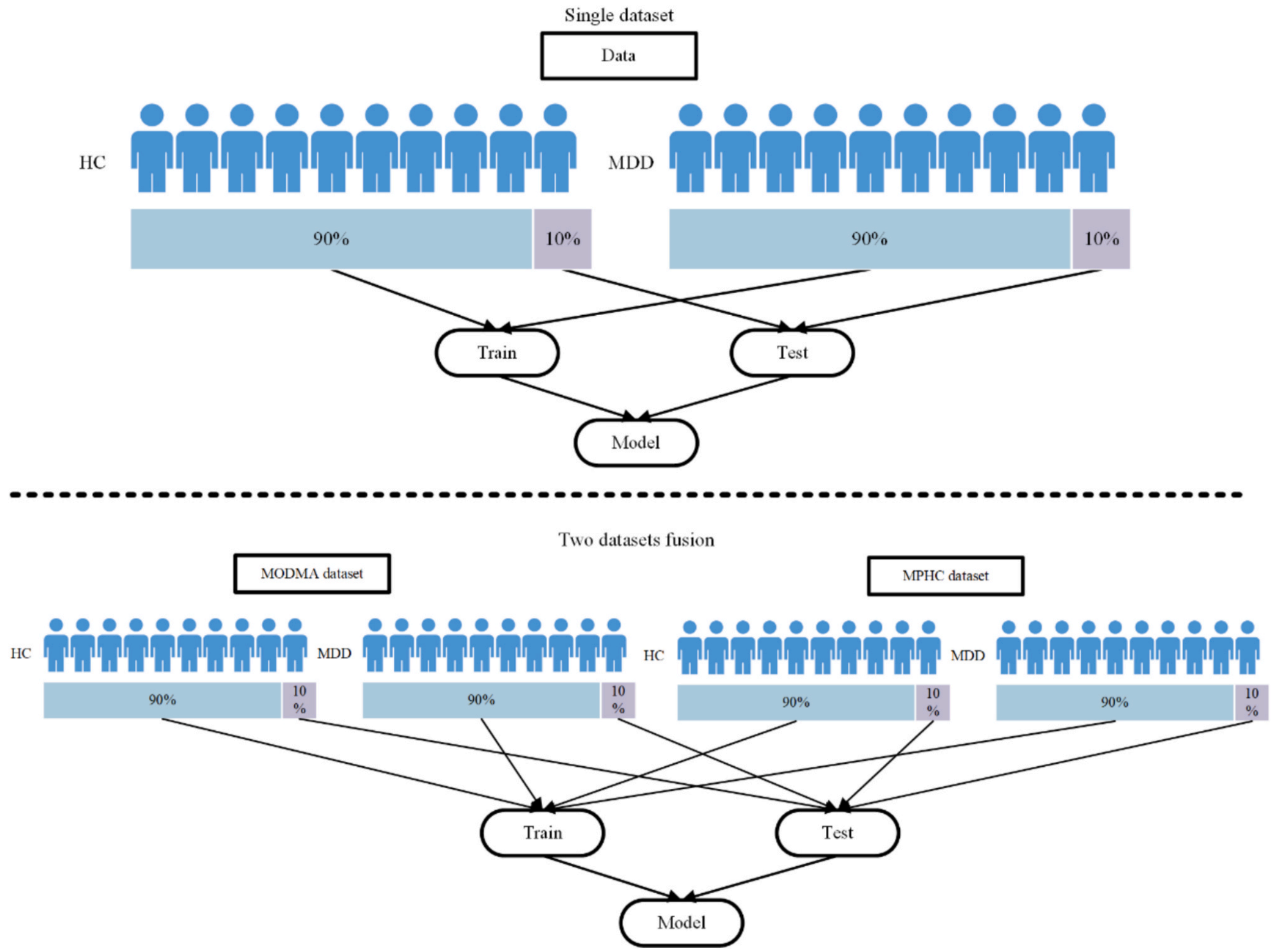

Fig. 3. Cross-subject experimental methods on single dataset or two datasets fusion.

randomly divided into 10 groups, and each time, the data of one of the groups of people is taken as the test set, and the data of the rest of the people is taken as the training set, until all the people's data serve as the test set, and the experiments are repeated for many times to get the results of the average index experiments.

(2) For the cross-subject experiment on the two datasets fusion, the data of 29 hc and 24 MDD in MODMA and 25 HC and 24 MDD in MPHC were included. The HC and MDD in both datasets were randomized into 10 groups. The first group of HC and the first group of MDD were combined into a test set, and the remaining 9 groups of HC and MDD were combined into a training set, and the experimental results were recorded. Then the same operation was carried out for the second group, and the training data and test data were fed into the classifier for classification. Until the data of all people served as the test set. Repeat the experiment several times to get the average index experimental results.

SVM, KNN, and DT are robust to overfitting due to their inherent properties and our use of 10-fold cross-validation, where 9 groups train the model and 1 group tests it, repeated 10 times, ensuring generalization across subjects. After feature selection, 10-fold cross-validation is also used to prevent overfitting and ensure the stability of the model's performance.

The experiments were performed on a laptop computer with the following specifications: AMD Ryzen 9 7945HX with Radeon Graphics @2.50 GHz, 16 GB RAM, NVIDIA GeForce 4060 graphics card and 64-bit Windows 11 operating system. For the SVM, we chose the 'linear' kernel function with 'BoxConstraint' = 1. For the KNN, $k = 3$ and distance = 'euclidean'. For DT, criterion = "gini", max_depth = "none". Except for the above parameters, the rest are default parameters.

Results and discussion

Analysis of the mean multiscale EEG features of MDD

In this study, different step sizes were used to characterize the LZC values of the corresponding scales, and the LZC feature matrices at different scales were extracted from under the MODMA and MPHC datasets. The statistical table of brain complexity results in each scale is shown in Table 3 as follows, LZC represents the sum of brain LZC value, while others represent the sum of brain LZC values for the corresponding scales. The average feature values of each channel in the MODMA and MPHC datasets are displayed on brain topographic maps in Figs. 4 and 5, respectively. LZC represents the LZC feature topography, and the others represent the corresponding scale feature topography, respectively.

From the results of the above figures and table, we found that under both datasets presented that in low frequency scales, such as the delta scale, the difference between the MDD group and the HC group was small, and the difference between the scales was not large. However, in high frequency scale, such as gamma scale, the difference between the two groups became larger, and the complexity of brain activity in the HC group was higher than that in the MDD group. This suggests that in the resting state, the MDD group has abnormal high frequency brain activity, and the complexity of brain activity is generally lower than that of the HC group in the whole brain.

Single scale EEG feature classification

On the MODMA dataset, the LZC feature matrix extracted from the

Table 3
Brain complexity statistics table in each scale.

		LZC	delta	theta	alpha	beta	gamma
MODMA	HC	5.3477	11.8964	12.4355	12.7249	13.4848	14.3636
	MDD	6.4025	11.9913	12.3386	12.5653	13.3171	13.9271
MPHC	HC	8.2629	8.9559	9.3122	10.5509	11.1173	10.8621
	MDD	9.5526	9.7665	10.0218	10.2774	10.4723	9.4282

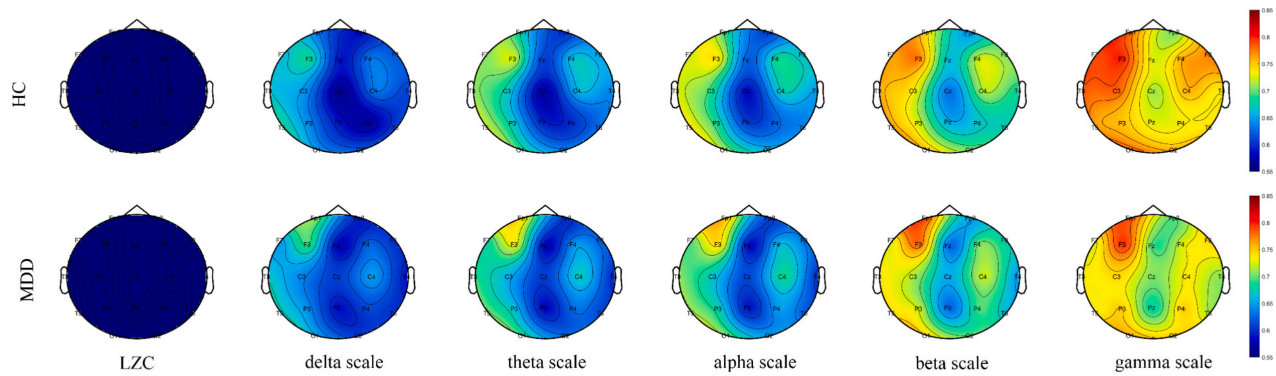

Fig. 4. Brain topography of LZC and each scale LZC in MODMA dataset.

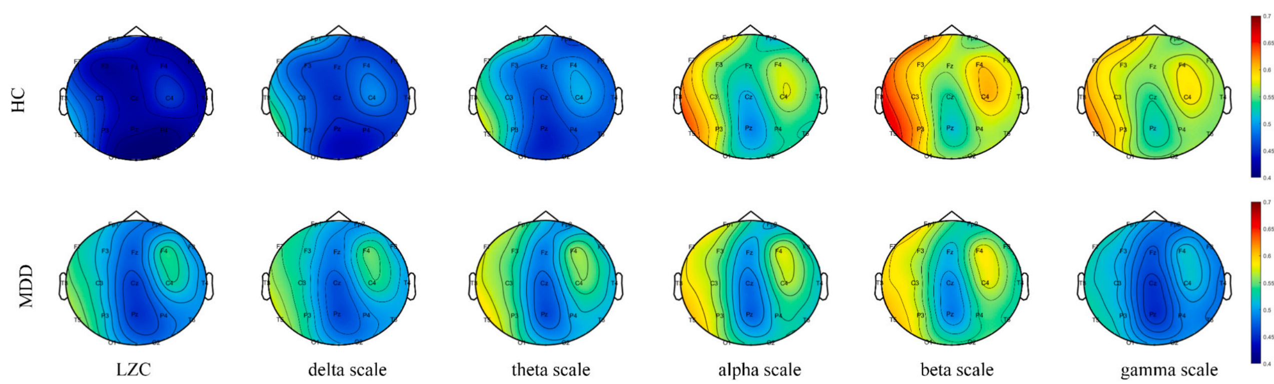

Fig. 5. Brain topography of LZC and each scale LZC in MPHC dataset.

MODMA dataset (MA_LZC) and the LZC feature matrix in each scale (MA_delta, etc.) were classified using SVM, KNN, and DT according to the cross-subjects experimental method. The classification results of the MODMA dataset are shown in Table 4.

From the table, it can be seen that the LZC feature classification results in beta and gamma scales are better than LZC and other low frequency scales. Among them, in gamma scale, the classification accuracy of 68.75 %, sensitivity of 71.39 % and specificity of 64.79 % were achieved on SVM classifier, which indicates that the complexity information of high frequency scale is better for the diagnosis of MDD.

On the MPHC dataset, the LZC feature matrix extracted from the MPHC dataset (MB_LZC) and the LZC feature matrix in each scale (MB_delta, etc.) were classified using SVM, KNN, and DT based on the cross-subjects experimental method. The classification results of the MPHC dataset are shown in Table 5.

From the table, it can be seen that the LZC feature classification results in each scale are better than LZC, and in beta and gamma scales are higher than other low frequency scales. Among them, in gamma scale, the classification accuracy of 73.44 %, sensitivity of 76.03 % and specificity of 70.20 % were achieved on SVM classifier, which indicates that the complexity information of high frequency scale is better for the diagnosis of MDD.

On the two datasets fusion, according to the cross-subject experimental method, SVM, KNN, and DT were used to classify LZC feature matrix (MC_LZC) extracted from the two datasets fused dataset and the LZC feature matrix (MC_delta, etc.) in each scale. The classification results of the two datasets fusion are shown in Table 6.

From the table, it can be seen that the LZC feature classification results in each scale are better than LZC, and in beta and gamma scales are higher than other low frequency scales. Among them, in gamma scale, the classification accuracy of 73.44 %, sensitivity of 76.03 % and specificity of 70.20 % were obtained on SVM classifier, which indicates that the complexity information of high frequency scale is better for the diagnosis of MDD.

Multiscale EEG feature fusion classification

We concatenated the LZC feature matrices in several scales to obtain the MLZC feature matrices MA_all, MB_all and MC_all on two datasets and two datasets fusion, respectively, at which time the dimension of the feature matrices became five times of the previous ones. Using the relief algorithm, irrelevant or redundant features are eliminated, and the importance of features for classification is evaluated by calculating the feature differences, and important features are selected to improve the

Table 4
Performance of LZC and each scale LZC on MODMA dataset.

feature	classifier	accuracy	sensitivity	specificity
MA_LZC	svm	62.67 %	63.33 %	61.67 %
	knn	57.85 %	67.62 %	48.08 %
	dt	56.78 %	62.12 %	51.43 %
MA_delta	svm	59.80 %	69.75 %	49.85 %
	knn	55.66 %	63.57 %	47.74 %
	dt	57.63 %	62.80 %	52.46 %
MA_theta	svm	57.07 %	65.50 %	48.64 %
	knn	52.25 %	59.13 %	45.38 %
	dt	53.00 %	57.83 %	48.17 %
MA_alpha	svm	57.53 %	67.43 %	47.62 %
	knn	51.64 %	58.83 %	44.45 %
	dt	51.12 %	57.84 %	44.39 %
MA_beta	svm	64.17 %	67.64 %	58.96 %
	knn	58.42 %	58.06 %	58.96 %
	dt	57.42 %	56.53 %	58.75 %
MA_gamma	svm	**68.75 %**	**71.39 %**	**64.79 %**
	knn	61.67 %	62.22 %	60.83 %
	dt	60.17 %	63.61 %	55.00 %

Table 5
Performance of LZC and each scale LZC on MPHC dataset.

feature	classifier	accuracy	sensitivity	specificity
MB_LZC	svm	77.06 %	78.09 %	76.02 %
	knn	68.61 %	59.41 %	77.81 %
	dt	68.88 %	67.35 %	70.40 %
MB_delta	svm	72.80 %	71.46 %	74.14 %
	knn	65.94 %	57.94 %	73.94 %
	dt	65.22 %	65.30 %	65.14 %
MB_theta	svm	69.25 %	67.55 %	70.94 %
	knn	62.02 %	52.02 %	72.03 %
	dt	62.63 %	62.90 %	62.37 %
MB_alpha	svm	70.89 %	65.49 %	76.36 %
	knn	66.47 %	57.32 %	75.62 %
	dt	65.73 %	66.06 %	65.39 %
MB_beta	svm	77.18 %	70.21 %	84.16 %
	knn	74.59 %	64.35 %	84.83 %
	dt	75.62 %	76.04 %	75.23 %
MB_gamma	svm	**82.61 %**	**78.36 %**	**86.86 %**
	knn	77.75 %	69.29 %	86.21 %
	dt	78.41 %	74.09 %	82.74 %

model performance. For comparison with LZC and each scale LZC, we chose to be consistent with them and retain the first 19 dimensional features. The results after relief feature selection on two datasets and two dataset fusion are shown in Table 7.

From the table, we can find that after feature selection, on two datasets and two datasets fusion, the most features were retained in gamma scale and mainly focuses on frontal lobe, temporal lobe, and central brain regions, which corresponds to the main brain regions discussed in the mean topography map, and these regions are of reference significance for the subsequent study of MDD. In addition to this, we found that the channel information in low frequency scale was also being preserved, which corresponded to the abnormalities in low frequency scales in the MDD group and the HC group mentioned in most studies (Wang et al., 2012). Finally, we obtained the new feature matrices MA_relief, MB_relief and MC_relief through selecting, which facilitated the subsequent comparison of classification effects.

Table 6
Performance of LZC and each scale LZC on two datasets fusion.

feature	classifier	accuracy	sensitivity	specificity
MC_LZC	svm	63.56 %	65.95 %	60.56 %
	knn	62.99 %	62.18 %	64.01 %
	dt	62.46 %	63.44 %	61.24 %
MC_delta	svm	67.36 %	73.43 %	59.77 %
	knn	59.42 %	58.36 %	60.75 %
	dt	59.40 %	61.35 %	56.96 %
MC_theta	svm	67.75 %	74.61 %	59.17 %
	knn	57.19 %	56.08 %	58.57 %
	dt	58.02 %	61.19 %	54.05 %
MC_alpha	svm	62.19 %	64.63 %	59.15 %
	knn	57.57 %	55.84 %	59.74 %
	dt	59.76 %	61.83 %	57.18 %
MC_beta	svm	69.02 %	70.60 %	67.04 %
	knn	63.04 %	60.30 %	66.46 %
	dt	65.97 %	68.52 %	62.78 %
MC_gamma	svm	**73.44 %**	**76.03 %**	**70.20 %**
	knn	66.03 %	64.78 %	67.58 %
	dt	66.60 %	65.30 %	68.22 %

Table 7
MLZC feature selection results.

dataset	feature selection	proportion of each region
MODMA	delta(Fp2 F4 C3 Cz O2) theta (Fp2 Cz) alpha(Fp2 Cz) beta (Fp2 Cz) gamma(Fp2 F4 T3 T5 C4 Fz Cz P3)	Frontal(36.83 %) Temporal (10.53 %) **Central(42.11 %)** Parietal-Occipital (10.53 %)
MPHC	delta(T5 O1) theta(C4 Fz O1) alpha(Fz) beta(T3 T5 Fz) gamma(Fp1 F3 F7 F8 T3 T4 T5 Fz O1 O2)	Frontal(10.53 %) **Temporal (42.11 %)** Central(26.3 %) Parietal-Occipital (21.06 %)
MODMA + MPHC	delta(Cz) theta(Fz Cz) alpha (Fp2 Fz Cz) beta(Fp2 T5 Fz Cz) gamma(Fp2 F4 T3 T5 C4 Fz Cz P3 O2)	Frontal(21.06 %) Temporal (15.78 %) **Central(52.63 %)** Parietal-Occipital (10.53 %)

According to the cross-subject experimental method, the MLZC concatenation matrix and the MLZC fusion matrix after relief feature selection were classified using SVM, KNN, and DT. The classification results are shown in Table 8.

From the table, it can be found that after feature selection, it presents better classification effects on all three datasets, which are all better than those in the full scale. It indicates that some brain area EEG activity complexity features selected in specific scales after relief feature selection have better and more stable effects on MDD diagnosis.

And from the table we can see that the feature effects after selection are all optimized on SVM. Both in each scale and multiscale fusion, the SVM effect is excellent. We compare the classification effects of LZC, optimal scale LZC, MLZC concatenation, and MLZC fusion and selection (MLZC-FS) obtained by SVM on two datasets and two datasets fusion, and the bar figure is shown in Fig. 6.

From the figure we can find that on different datasets, the effect of LZC in high frequency scale is better than LZC, but after concatenating all scale MLZC features, the effect is lower than optimal scale LZC

Table 8
Performance of MLZC-FS and MLZC concatenation.

feature	classifier	accuracy	sensitivity	specificity
MA_relief	svm	72.42 %	75.56 %	67.71 %
	knn	68.67 %	74.17 %	60.42 %
	dt	63.83 %	67.92 %	57.71 %
MB_relief	svm	**84.81 %**	**80.02 %**	**89.60 %**
	knn	83.45 %	77.54 %	89.37 %
	dt	78.45 %	77.67 %	79.82 %
MC_relief	svm	76.13 %	77.58 %	74.31 %
	knn	71.49 %	71.06 %	72.02 %
	dt	68.47 %	68.58 %	68.33 %
MA_all	svm	67.42 %	68.47 %	65.83 %
	knn	63.25 %	63.61 %	62.71 %
	dt	59.17 %	58.47 %	60.21 %
MB_all	svm	82.47 %	80.85 %	84.10 %
	knn	80.77 %	79.03 %	82.51 %
	dt	78.15 %	77.79 %	78.50 %
MC_all	svm	70.90 %	72.44 %	68.96 %
	knn	68.07 %	69.69 %	66.05 %
	dt	67.78 %	68.34 %	67.05 %

instead, probably because of the more irrelevant features due to feature redundancy, which affects the classification accuracy. After we used the feature selection, the classification effect on two datasets and two datasets fusion improved significantly; on MODMA, achieved 72.42 % classification accuracy; on MPHC, achieved 84.81 % classification accuracy; and on the two datasets fusion, achieved 76.13 % classification accuracy. These results indicate that MLZC-FS can integrate channel information from different frequency bands, then relief feature screening can effectively reduce redundant information and noise, and improve the detection performance for MDD.

Discussion

Compared with LZC, MLZC reflects the nonlinear characteristics of EEG signals of MDD more comprehensively by capturing changes in signal complexity at different scales. Conventional LZC is prone to overlook the subtle changes in high-rate brain activity due to the singularity of the binarization threshold. By introducing different smoothing windows, the multiscale method not only enhances the ability to capture fast oscillations, but also retains the sensitivity to low frequency bands of activities, which makes it more suitable for the analysis of complex EEG signals.

From the mean brain topography, it was shown that on both datasets, the difference in low frequency scales was not obvious, the difference in high frequency scales became larger, and the complexity of brain activities in depressed patients was generally lower than that in healthy people. After feature selecting, we found that the frontal, temporal and central brain regions had higher weights in the diagnostic questions, indicating that the complexity of activity in these brain regions in depressed patients is different from that of normal controls, which is consistent with the literature (Yang et al., 2023).

From the comparative analysis of each scale LZC with the LZC, we found that the gamma scale LZC features were significantly better than LZC methods and low frequency scale segment features in terms of classification accuracy. Some studies have shown that people with MDD experience abnormal changes in the gamma waves of EEG signals in the frontal and temporal regions compared to normal people (Strelets et al., 2007). Therefore, the validity of the gamma scale LZC features in this study further supports the importance of gamma band information in MDD research.

We see from the results of feature selecting that there are EEG channel features in all scales play a role in the classification, of which the higher number is still in the high frequency scale, especially the gamma scale, which verifies the importance of the information on the complexity of the high frequency band of EEG activity for the diagnosis of MDD under the resting state with eyes closed in addition to information on the brain activity in the low frequency band. Combined with the results of the histogram analysis in Fig. 6, our proposed MLZC-FS analysis method retains the high frequency scale features that are more effective for the diagnostic problem, reduces feature redundancy, and also better contains the changes in the complexity of the brain activity under each frequency band, resulting in a better classification effect.

From the above diagnostic results, the MLZC-FS method has strong

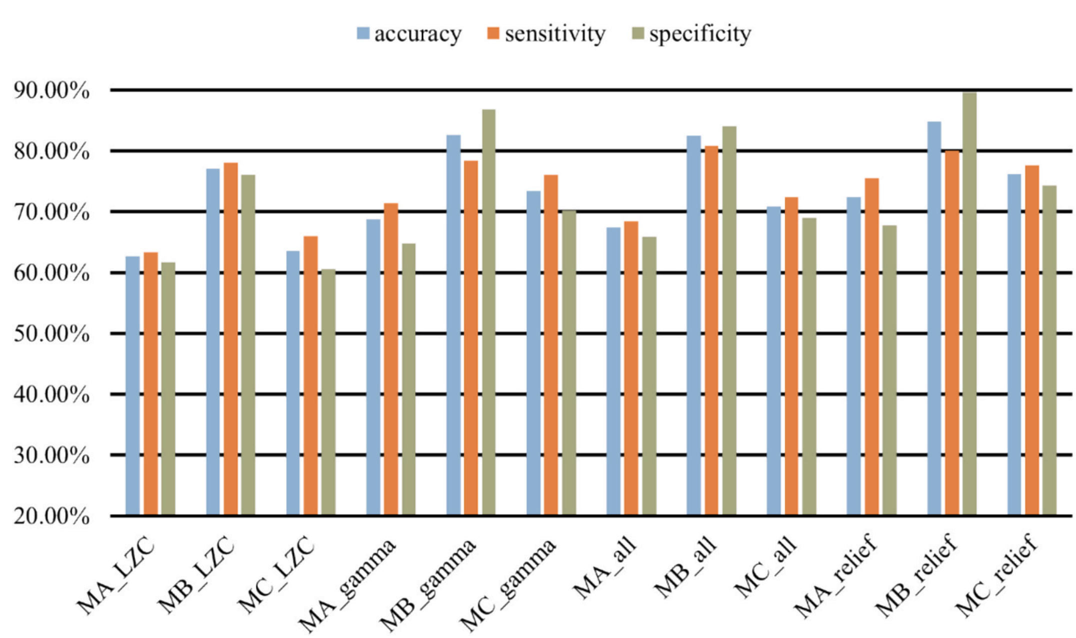

Fig. 6. Performance of LZC, optimal scale LZC, MLZC concatenation and MLZC-FS.

cross-subject diagnostic ability. The better diagnostic results on different datasets show that the method is robust and the results are stable and reliable. Compared with deep learning, MLZC-FS provides lower computational complexity, higher interpretability, and better performance on small datasets, rather than deep learning methods that require a large amount of data.

We also compared the method with some of the recent research (Yang et al., 2023; Yang et al., 2023), under the eye close paradigm of MPHC, Yang et al. (2023) searched for the optimal combination of brain regions by combining different brain regions, and the final classification accuracy under resting state with eye close was 81.7 %. In another study (Yang et al., 2023), high cross-subject classification accuracy was achieved by fusing the feature matrices of the resting states with eyes open and eyes closed, where a cross-subject classification accuracy of 77.32 % was obtained in the resting state with eyes closed. Upon comparison, it was found that the MLZC-FS method proposed in this study achieved a high cross-subject classification accuracy of 84.81 % classification accuracy in the resting state with eyes closed. On MODMA dataset, Mao et al. (2024) used a Generative Detection network (GDN) method by training two generators to learn the brain activity characteristics of depressed patients and healthy controls, and the diagnostic accuracy of 92.30 % was obtained in the trained model. Shen et al. (2023) proposed an interpretable graph-convolutional network to extract spatial–temporal features of EEG signals for MDD diagnostic analysis, and finally achieved a classification accuracy of 76.5 %. Comparing with existing studies (Mao et al., 2024; Shen et al., 2023), although our classification effect is lower than some existing studies, in contrast, this study only used EEG data from 19 electrodes and ultimately used only 19-dimensional features for classification experiments under the SVM classifier, which is simpler and easier to deploy compared to deep learning; moreover, we improved the classification accuracy by 9.57 % on the basis of the LZC; Finally, this study does cross-subject diagnosis, which is more suitable for the clinical application of MDD diagnosis. On two datasets fusion, Sun et al. (2024) conducted a cross-dataset test to evaluate the generalizability of their proposed graph neural network model for MDD detection. When trained on the Distress Analysis Interview Corpus-Wizard of Oz (DAIC-WOZ) dataset and tested on the MODMA dataset, the model achieved an accuracy of 48.72 %, in contrast to training on the MODMA dataset and testing on the DAIC-WOZ dataset with an accuracy of 61.64 %. We fused these two datasets, MODMA and MPHC, and conducted cross-subject experiments, achieving a high classification accuracy of 76.13 % on SVM, which improves the classification accuracy by 12.57 % compared to LZC analysis method, and realizes the multi datasets fusion cross-subject MDD diagnosis, which shows the excellence and stability of the multi-scale feature classification method proposed in this paper.

Conclusions

In this study, MLZC-FS method is proposed for the diagnosis of cross-subject MDD patients for depressed EEG signals in the resting state. In this study, it was found that the LZC values of MDD patients were higher than those of HC, but showed different performances at different scales. Specifically, in low scales, the eigenvalues in the MDD were higher than those in the HC, but in high scales, we found the MDD to be lower than the HC. The different complexity changes also represented different brain electrical activities, indicating the necessity of nonlinear feature research in different frequency bands. Previous studies on the resting-state EEG of MDD patients have largely ignored the gamma frequency band and the nonlinear features of EEG signals. This study demonstrates that MLZC effectively captures the nonlinear features across different frequency bands in EEG signals, highlighting its potential as an important tool for future research in this domain. Through the analysis of each scale LZC, it is proved that the complexity features in the high frequency scale, especially in the gamma scale, are more effective for the diagnosis of MDD, which indicates that the complexity information in the high frequency scale of EEG signal is more effective for the diagnosis of MDD. After MLZC-FS, more complexity features of gamma scale channels were retained after selecting, which also verified the importance of high frequency information for MDD diagnosis. In summary, the MLZC-FS method proposed in this study finds an effective method for cross-subject diagnosis of MDD in the resting state, which is robust and can effectively improve the accuracy of MDD diagnosis on all three datasets. The two datasets used in this paper are both in the resting state with eyes closed, and this paradigm is easy to implement in a clinical setting, thus assisting in the clinical diagnosis and treatment of MDD patients.

Of course, there are some limitations in this study, such as the step size chosen in selecting the LZC of the corresponding scale is only roughly representative of the information in the band, and does not fully utilize all the information in the band effectively. In addition, when this paper conducts feature selecting, in order to compare with the other methods, it chooses the same feature dimension, which is not guaranteed to be the optimal feature dimension for diagnosis. And the study only used 19 electrodes, which has certain limitations for whole-brain range analysis. Finally, the amount of data is still small overall, and more resting state EEG datasets can be added in the future to test the effect of multiscale complexity features on MDD diagnosis.

Ethics statement

We ensure that all procedures are in compliance with relevant laws and institutional guidelines. We use publicly available datasets where the datas do not contain any identifying markers and do not contain any text that could identify the individual in question. These datasets have been ethically approved for research purposes, so no ethical claims are required.

CRediT authorship contribution statement

Zhen Zhang: Writing – original draft, Visualization. **Jianli Yang:** Writing – review & editing. **Peng Xiong:** Writing – review & editing, Conceptualization. **Huaqing Hao:** Data curation. **Jieshuo Zhang:** Investigation. **Licong Li:** Writing – review & editing. **Changyong Wang:** Supervision, Project administration. **Xiuling Liu:** Writing – review & editing, Funding acquisition, Conceptualization.

Funding

This work was supported by Expert Recommended Original Exploration Project (62450100), the major research instrument development project of the National Natural Science Foundation of China (Grant No. 82327810), the Interdisciplinary Research Program of Natural Science of Hebei University (DXK202205), and the National Natural Science Foundation of China (62276087, 62403180).

Declaration of competing interest

The authors declare that they have no known competing financial interests or personal relationships that could have appeared to influence the work reported in this paper.

References

Dimitri Marques Abramov, Henrique Santos Lima, Vladimir Lazarev, Paulo Ricardo Galhanone, Constantino Tsallis, Identifying attention-deficit/hyperactivity disorder through the electroencephalogram complexity, Physica A: Statistical Mechanics and its Applications, Volume 653, 2024, 130093, ISSN 0378-4371, https://doi.org/10.1016/j.physa.2024.130093.

Angulo-Ruiz, B.Y., Ruiz-Martínez, F.J., Rodríguez-Martínez, E.I., Ionescu, A., Saldaña, D., Gómez, C.M., 2023. Linear and Non-linear analyses of EEG in a Group of ASD Children during resting state condition. Brain Topogr. 36 (5), 736–749. https://doi.org/10.1007/s10548-023-00976-7.

Angulo-Ruiz, B.Y., Muñoz, V., Rodríguez-Martínez, E.I., Cabello-Navarro, C., Gómez, C. M., 2023. Multiscale entropy of ADHD children during resting state condition. Cogn. Neurodyn. 17 (4), 869–891. https://doi.org/10.1007/s11571-022-09869-0.

Anik, I.A., Kamal, A., Kabir, M.A., Uddin, S., Moni, M., 2024. A robust deep-learning model to detect major depressive disorder utilizing EEG signals. IEEE Trans. Artif. Intell. 5 (10), 4938–4947. https://doi.org/10.1109/TAI.2024.3394792.

Cai, H., Yuan, Z., Gao, Y., et al., 2022. A multi-modal open dataset for mental-disorder analysis. Sci. Data 9, 178. https://doi.org/10.1038/s41597-022-01211-x.

Cortes, C., Vapnik, V., 1995. Support-vector networks. Mach. Learn. 20 (3), 273–297. https://doi.org/10.1007/BF00994018.

Cover, T.M., Hart, P.E., 1967. Nearest neighbor pattern classification. IEEE Trans. Inf. Theory 13 (1), 21–27. https://doi.org/10.1109/TIT.1967.1053964.

COVID-19 Mental Disorders Collaborators. (2021). Global prevalence and burden of depressive and anxiety disorders in 204 countries and territories in 2020 due to the COVID-19 pandemic. Lancet, 398(10312), 1665-1666. DOI: 10.1016/S0140-6736(21)02221-2.

He, Y., Guo, W., Ren, Z., Liu, S., Ming, D., 2023. Gamma rhythm and theta-gamma coupling alternation in chronic unpredictable stress (CUS)-induced depression rats. In: 2023 45th Annual International Conference of the IEEE Engineering in Medicine & Biology Society (EMBC), pp. 1–4. https://doi.org/10.1109/EMBC40787.2023.10340209.

Ibáñez-Molina, A., Iglesias-Parro, S., Soriano, M.F., Aznarte, J., 2015. Multiscale Lempel-Ziv complexity for EEG measures. Clin. Neurophysiol. 126 (3), 541–548. https://doi.org/10.1016/j.clinph.2014.07.012.

Kaspar, F., Schuster, H.G., 1987. Easily calculable measure for the complexity of spatiotemporal patterns. Phys. Rev. A 36 (2), 842–848. https://doi.org/10.1103/PhysRevA.36.842.

Ke, S., Li, Y., Huang, X., Chen, Z., 2024. Multi-region and multi-band electroencephalogram emotion recognition based on self-attention and capsule network. Neural Netw. 155, 34–45. https://doi.org/10.1016/j.neunet.2023.10.004.

Kononenko, I. (1994). Estimating attributes: Analysis and extensions of RELIEF. In F. Bergadano & L. De Raedt (Eds.), Machine learning: ECML-94 (Lecture Notes in Computer Science, 784, 171-182. Springer. DOI: 10.1007/3-540-57868-4_57.

Lan, Y.-T., Peng, D., Liu, W., et al., 2023. Investigating Emotion EEG patterns for Depression Detection with Attentive simple Graph Convolutional Network. In: 2023 45th Annual International Conference of the IEEE Engineering in Medicine & Biology Society (EMBC), pp. 1–4. https://doi.org/10.1109/EMBC40787.2023.10340623.

Lempel, A., Ziv, J., 1976. On the complexity of finite sequences. IEEE Trans. Inf. Theory 22 (1), 75–81. https://doi.org/10.1109/TIT.1976.1055501.

Li, C., Li, P., Zhang, Y., et al. (2024). Effective Emotion Recognition by Learning Discriminative Graph Topologies in EEG Brain Networks. IEEE Transactions on Neural Networks and Learning Systems, 35(8), 10258-10272. https://doi.org/10.1109/TNNLS.2023.3238519.

Liang, M., Lomayesva, S., Isham, E.A., 2022. Dissociable Roles of Theta and Alpha in Sub-second and Supra-Second Time Reproduction: an Investigation of their Links to Depression and anxiety. Timing Time Percept. 11 (1–4), 322–342. https://doi.org/10.1163/22134468-bja10061.

Lord, B., Allen, J.J.B., 2023. Evaluating EEG complexity metrics as biomarkers for depression. Psychophysiology 60 (8), e14274. https://doi.org/10.1111/psyp.14274.

Luo, Y., Tang, M., Fan, X., 2025. Meta analysis of resting frontal alpha asymmetry as a biomarker of depression. Npj Mental Health Res 4, 2. https://doi.org/10.1038/s44184-025-00117-x.

Maddirala, A.K., Shaik, R.A., 2018. Separation of sources from Single-Channel EEG Signals using Independent Component Analysis. IEEE Trans. Instrum. Meas. 67 (2), 382–393. https://doi.org/10.1109/TIM.2017.2775358.

Malhi, G.S., Mann, J.J., 2018. Depression. Lancet 392 (10161), 2299–2312. https://doi.org/10.1016/S0140-6736(18)31948-2.

Mao, Z., Wu, H., Tan, Y., & Jin, Y. (2024). EEG based generative depression discriminator. arXiv preprint arXiv:2402.09421. DOI: 10.48550/arXiv.2402.09421.

Mumtaz, W., Xia, L., Mohd Yasin, M.A., Azhar Ali, S.S., Malik, A.S., 2017. A wavelet-based technique to predict treatment outcome for Major Depressive Disorder. PLoS One 12 (2), e0171409. https://doi.org/10.1371/journal.pone.0171409.

Pratiwi, M., 2023. Comparative analysis of brain waves for EEG-based depression detection in the prefrontal cortex lobe using LSTM. In: Proceedings of the 2023 7th International Conference on New Media Studies (CONMEDIA), pp. 173–178. https://doi.org/10.1109/CONMEDIA60526.2023.10428546.

Quinlan, J.R., 1986. Induction of decision trees. Mach. Learn. 1 (1), 81–106. https://doi.org/10.1007/BF00116251.

Shen, J., Chen, J., Ma, Y., Cao, Z., Zhang, Y., Hu, B., 2023. Explainable depression recognition from EEG signals via graph convolutional network. In: In 2023 IEEE International Conference on Bioinformatics and Biomedicine (BIBM), pp. 1406–1412. https://doi.org/10.1109/BIBM58861.2023.10386011.

Strelets, V.B., Garakh, Z.V., Novototskii-Vlasov, V.Y., 2007. Comparative study of the gamma rhythm in normal conditions, during examination stress, and in patients with first depressive episode. Neurosci. Behav. Physiol. 37 (4), 387–394. https://doi.org/10.1007/s11055-007-0025-4.

Sun, C., Jiang, M., Gao, L., Xin, Y., Dong, Y., 2024. A novel study for depression detecting using audio signals based on graph neural network. Biomed. Signal Process. Control 84, 104987. https://doi.org/10.1016/j.bspc.2023.104987.

Sun, H., Mao, S., Cai, W., et al., 2025. BISNN: Bio-information-fused spiking neural networks for enhanced EEG-based emotion recognition. Cogn. Neurodyn. 19, 52. https://doi.org/10.1007/s11571-025-10239-9.

Tatti, E., Cinti, A., Serbina, A., Luciani, A., D'Urso, G., Cacciola, A., Quartarone, A., Ghilardi, M., 2024. Resting-state EEG alterations of practice-related spectral activity and connectivity patterns in depression. Biomedicines 12 (9), 2054. https://doi.org/10.3390/biomedicines12092054.

Wang, L., Dai, W., Su, Y., Wang, G., Tan, Y., 2012. Amplitude of low-frequency oscillations in first-episode, treatment-naive patients with major depressive disorder: a resting-state functional MRI study. PLoS One 7 (10), e48658. https://doi.org/10.1371/journal.pone.0048658.

Wang, H.G., Li, M., Zhao, X., 2023. AMGCN-L: an adaptive multi-time-window graph convolutional network with long-short-term memory for depression detection. IEEE Trans. Biomed. Eng. 70 (7), 2203–2216. https://doi.org/10.1109/TBME.2023.3255687.

Xu, C., Zhang, J., Wang, Y., Liu, X., 2024. An EEG-based depressive detection network with adaptive feature learning and channel activation. IEEE Trans. Neural Syst. Rehabil. Eng. 32 (4), 563–574. https://doi.org/10.1109/TNSRE.2024.3125945.

Yang, K., Hu, Y., Zeng, Y., et al., 2023. EEG network analysis of depressive emotion interference spatial cognition based on a simulated robotic arm docking task. Brain Sci. 14 (1), 44. https://doi.org/10.3390/brainsci14010044.

Yang, J., Zhang, Z., Fu, Z., Li, B., Xiong, P., Liu, X., 2023. Cross-subject classification of depression by using multiparadigm EEG feature fusion. Comput. Methods Programs Biomed. 236, 107534. https://doi.org/10.1016/j.cmpb.2023.107534.

Yang, J., Zhang, Z., Xiong, P., Liu, X., 2023. Depression detection based on analysis of EEG signals in multi brain regions. J. Integr. Neurosci. 22 (4), 93. https://doi.org/10.31083/j.jin2204093.

Zhang, W., Liu, W., Liu, X., et al., 2022. Altered lateralization of gamma oscillations and theta-gamma coupling in major depression: an eeg study. ACM Trans. 203–208. https://doi.org/10.1145/3574198.3574230.

Zhu, J., Li, X., Hou, P., Hu, B., Zhang, X., 2023. EEG-based depression recognition using convolutional neural network with FFT and EMD. IEEE International Conference on Bioinformatics and Biomedicine (BIBM) 2023, 2601–2608. https://doi.org/10.1109/BIBM58861.2023.10385385.

Zimmerman, M., Ellison, W., Young, D., Chelminski, I., Dalrymple, K., 2015. How many different ways do patients meet the diagnostic criteria for major depressive disorder? Compr. Psychiatry 56, 29–34. https://doi.org/10.1016/j.comppsych.2014.09.007.